Bilal R. Kaafarani, Brigitte Wex, Bernd Strehmel,
Douglas C. Neckers

Structural concept for fluorinated Y-enynes with solvatochromic properties

first published in:
Photochemical and Photobiological Sciences - 1 (2002), p. 942-950
ISSN: 1474-905X
DOI: 10.1039/b208326d

PPS
Paper
www.rsc.org/pps

Structural concept for fluorinated Y-enynes with solvatochromic properties[1] †

Bilal R. Kaafarani,[a] Brigitte Wex,[a] Bernd Strehmel[b] and Douglas C. Neckers*[a]

[a] *Center for Photochemical Sciences, Bowling Green State University, Bowling Green, OH 43403, USA. E-mail: neckers@photo.bgsu.edu; Tel: +419-372-2034*
[b] *Institute of Chemistry, Physical Chemistry, University of Potsdam, Karl-Liebknecht Str. 24/25, D-14476 Golm, Germany*

Received 28th August 2002, Accepted 14th October 2002
First published as an Advance Article on the web 5th November 2002

An approach to the development of fluorescent probes to follow polymerizations *in situ* using fluorinated cross-conjugated enediynes (Y-enynes) is reported. Different substitution patterns in the Y-enynes result in distinct solvatochromic behavior. β,β-Bis(phenylethynyl)pentafluorostyrene **7**, which bears no donor substituents and only fluorine at the styrene moiety, shows no solvatochromism. Donor substituted β,β-bis(3,4,5-trimethoxyphenylethynyl)pentafluorostyrene **8** and β,β-bis(4-butyl-2,3,5,6-tetrafluorophenylethynyl)-3,4,5-trimethoxystyrene **9** exhibit solvatochromism upon change of solvent polarity. Y-enyne **8** showed the largest solvatochromic shift (94 nm bathochromic shift) upon changing solvent from cyclohexane to acetonitrile. A smaller solvatochromic response (44 nm bathochromic shift) was observed for **9**. Lippert–Mataga treatment of **8** and **9** yields slopes of −10,800 and −6,400 cm^{-1}, respectively. This corresponds to a change in dipole moment of 9.6 and 6.9 D, respectively. The solvatochromic behavior in **8** and **9** supports the formation of an intramolecular charge transfer (ICT) state. The low fluorescence quantum yields are caused by competitive double bond rotation. The fluorescence decay time of **9** decreases in methyltetrahydrofuran from 2.1 ns at 77 K to 0.11 ns at 200 K. Efficient single bond rotation in **9** was frozen at −50 °C in a configuration in which the trimethoxyphenyl ring is perpendicular to the fluorinated rings. **7**–**9** are photostable compounds. The X-ray structure of **7** shows it is not planar and that its conjugation is distorted. Y-enyne **7** stacks in the solid state showing coulombic, actetylene–arene, and fluorine–π interactions.

Introduction

Solvatochromism is the response in the absorption or emission spectrum of a molecule upon changing the solvent polarity.[2] The emission maximum of molecules with relatively low dipole moments in the ground state but large dipole moments in the excited state, due to intramolecular charge transfer (**ICT**), shift to longer wavelengths (bathochromic shift) as the polarity of the solvent increases. This is due to the fact that stabilization of the dipolar excited state is larger in more polar solvents.[3,4] Polymerization processes lead to large changes in the mobility of the medium. As a result, compounds whose fluorescence is sensitive to such changes can be used as indicators of the degree of polymerization.[5c] Fluorescent probes have been extensively used in our laboratory to monitor polymerization,[3,5] and certain solvatochromic molecules have been used in radiation cure technology.[6] As polymerization increases, the viscosity of the environment increases leading to a blue shift in the emission of the probe.[3,4]

Cross-conjugated enediynes (Y-enynes) have recently attracted considerable attention because they display reduced π-electron delocalization and this affects the degree of electronic communication. They are therefore useful in several electronic and photonic applications.[7,8] Introduction of more than one fluorine atom into the Y-enyne skeleton results in a highly sensitive system exhibiting extraordinary photonic properties, *i.e.* solvatochromism.[4,9–11] Recently the polarity dependent emission of substituted tetraethynylethene was reported.[12] In this paper, we report the first approach to develop fluorescent probes from fluorinated cross-conjugated systems.

† This paper is dedicated to Professor Dr J. W. Neckers on the occasion of his 100th birthday.

Experimental

General

All manipulations were performed under argon. Reagents were purchased from Aldrich and used without further purification. Spectroscopic solvents were purchased from Aldrich and VWR and used without further purification. Methylene chloride was dried over CaH_2; THF was dried over sodium. ^1H and ^{19}F NMR spectra were recorded with either a Varian Gemini 200 NMR or a Varian Unity plus 400 NMR spectrometer. Chemical shifts are reported in ppm with TMS as the internal standard (^1H NMR) or $CFCl_3$ as the external standard (^{19}F NMR). MS measurements were carried out on a Shimadzu GCMS-QP5050 mass spectrometer equipped with a DI-50 direct sample inlet device. UV–VIS spectra were recorded on a HP 8452A diode array UV–VIS spectrometer. High-resolution mass spectra were obtained from the Mass Spectrometry Laboratory in the University of Illinois at Urbana-Champaign. Element analysis was performed at Atlantic Microlab, Inc. Thin-layer chromatography was performed on Sorbent Technologies plates (layer thickness 250 μm, particle size 5–17 μm, pore size 60 Å). Silica gel chromatography was performed using silica gel (40 μm, 32–63 μ) purchased from Sorbent Technologies Inc. Melting points were determined using a capillary melting point apparatus (Uni-melt, Arthur H. Thomas Co., Philadelphia, PA) and were uncorrected.

Fluorescence spectra were recorded with a Spex Fluorolog 2 equipped with both excitation and emission double-beam monochromators. All spectra were corrected and were measured in perpendicular geometry using 1 cm quartz cuvettes. Fluorescence quantum yields are relative to anthracene in ethanol as the external standard (φ_f = 0.27 in

 DOI: 10.1039/b208326d

ethanol[13]) for **7** and **8** and 9,10-dimethylanthracene ($\varphi_f = 0.9$ in cyclohexane[14]) for **9**. All solutions were degassed with argon for 6 minutes.

Synthesis

β,β-Dibromopentafluorostyrene [2]. This compound was synthesized using a modification of a literature procedure.[15] Pentafluorobenzaldehyde **1** (10.0 g, 51.0 mmol) and triphenylphosphine (28.1 g, 107 mmol) were dissolved in 150 ml freshly distilled CH_2Cl_2. CBr_4 (18.6 g, 56.1 mmol) was dissolved in 50.0 ml CH_2Cl_2 and placed in a dropping funnel. The setup was degassed with argon. The CBr_4 solution was added at a steady rate into the reaction mixture which was stirred under argon for three hours at 0 °C. The reaction mixture was then stirred for two hours at room temperature, poured in 500 ml of petroleum ether, filtered and evaporated on a rotary evaporator. The residue, β,β-dibromopentafluorostyrene **2** contaminated with triphenylphosphine oxide, was stirred with hexanes (to separate **2** from triphenylphosphine oxide), filtered and then evaporated. This process was repeated until no more **2** was present in the residue. Alternatively, **2** could be purified by running through a column of silica gel. 9.50 g of β,β-dibromopentafluorostyrene **2** (53%) were isolated. This compound was used without further purification. ^{1}H NMR (200 MHz, $CDCl_3$): δ 6.03 (br s, 1 H). ^{19}F NMR (376 MHz, $CDCl_3$): δ −137. 97 (br s, 2F), −153.39 (br s, 1F), −162.12 (br s, 2F).

1-Ethynyl-4-butyltetrafluorobenzene [3]. This compound was synthesized using a modification of a literature procedure.[16] β,β-Dibromopentafluorostyrene **2** (6.00 g, 17.0 mmol) was dissolved in 100 ml freshly distilled THF. In a dropping funnel, n-BuLi (20.0 ml, 51.0 mmol, 2.50 M in hexanes) was placed. The reaction vessel was placed in a Dewar flask (−78 °C) and degassed with argon. n-BuLi was added slowly and the reaction mixture stirred under argon at −78 °C for three hours, then at room temperature for two hours. The reaction mixture was poured then into 100 ml of saturated NH_4Cl and extracted with 3 × 100 ml of diethyl ether. The ether layers were combined and evaporated to yield 1-ethynyl-4-butyltetrafluorobenzene **3**, which was then distilled at 8×10^{-3} Torr; 3.33 g were isolated (85%). The compound was used without further purification. ^{1}H NMR (200 MHz, $CDCl_3$): δ 0.90–0.97 (t, 3 H), 1.26–1.46 (septet, 2H), 1.51–1.66 (pentet, 2H), 2.69–2.78 (t, 2H), 3.58 (s, 1 H). ^{19}F NMR (376 MHz, $CDCl_3$): −138.42 (t, 2F), −154.17 (t, 2F).

β,β-Dibromo-3,4,5-trimethoxystyrene [5]. The title compound was synthesized by the same method as was **2** however 3,4,5-trimethoxybenzaldehyde **4**, was used as starting material. The product was used without further purification. ^{1}H NMR (200 MHz, $CDCl_3$): δ 3.87 (s, 9 H), 6.80 (s, 2 H), 7.41 (s, 1 H).

1-Ethynyl-3,4,5-trimethoxybenzene [6]. The title compound was synthesized using the same method as was **4** however β,β-dibromo-3,4,5-trimethoxystyrene **5**, was used as the starting material. The compound was used without further purification. ^{1}H NMR (200 MHz, $CDCl_3$): δ 3.04 (s, 1H), 3.86 (s, 9 H), 6.74 (s, 2 H).

β,β-Bis(phenylethynyl)pentafluorostyrene [7]. This compound was synthesized using a modification of a literature procedure.[17] β,β-Dibromopentafluorostyrene **2** (1.00 g, 2.86 mmol) was dissolved in 100 ml THF–NEt_3 (1 : 1). $Pd(PPh_3)_2Cl_2$ (200 mg, 0.280 mmol) and CuI (110 mg, 0.570 mmol) were then added. The reaction mixture was stirred under argon for 10 minutes. Phenylacetylene (700 mg, 6.86 mmol) was added slowly over a period of 1 hour to the reaction mixture through a septum. The reaction mixture was stirred under argon for 24 hours at 70 °C in an oil bath. After aqueous workup, the compound was subjected to a short column, then run over another column using hexane–ethyl acetate as eluent (Hex–EA; 9 : 1). The title compound (yellow solid) was isolated in 55% (622 mg): mp 135–137 °C. ^{1}H NMR (200 MHz, $CDCl_3$): δ 6.92–6.93 (dd, 1 H, $J_1 = 2.4$ Hz, $J_2 = 1.1$ Hz), 7.32–7.45 (m, 8 H), 7.54–7.59 (m, 2 H). ^{19}F NMR (376 MHz, $CDCl_3$): δ −136.2 (multiplet appearing as singlet, 2F), −154.2 (m, 1F), −162.9 (multiplet appearing as singlet, 2F). ^{13}C NMR (50 MHz, $CDCl_3$): δ 84.95 (C), 87.03 (C), 90.58 (C), 93.67 (C), 95.53 (C), 110.79–111.52 (C, dt, $J_1 = 3.3$, $J_2 = 17.3$ Hz), 121.97–122.07 (C, d, $J = 5.45$ Hz), 126.61 (CH), 129.08 (CH), 129.21 (CH), 129.41 (CH), 131.74 (CH), 131.88 (CH) and a series of broad peaks in the aromatic region (Ar C–F). HR–MS: calcd for *m*/*z* 394.078092, found *m*/*z* 394.077464.

β,β-Bis(3,4,5-trimethoxyphenylethynyl)pentafluorostyrene [8]. The title compound was synthesized using the same procedure as was **8** however β,β-dibromopentafluorostyrene **2** and 1-ethynyl-3,4,5-trimethoxybenzene **6**, were used as starting materials. After aqueous workup, the compound was subjected to a short column, then run over another column using hexane–ethyl acetate as eluent (Hex–EA; 2.5 : 1). The title compound (greenish solid) was isolated in 35% yield: mp 160–161 °C. ^{1}H NMR (400 MHz, $CDCl_3$): δ 3.86–3.90 (m, 18 H), the vinyl hydrogen was assigned to the broad singlet at 6.97 ppm (this is consistent with the vinyl hydrogen in **7**). The four aromatic hydrogens appear in repeated synthesis as singlets at 6.65, 6.76 and 6.80 ppm. ^{19}F NMR (376 MHz, $CDCl_3$): δ (−136.00)–(−135.96) (d, 2F, $J = 18$ Hz), (−154.24)–(−154.12) (t, 1F), (−163.13)–(−163.03) (t, 2F).^{13}C NMR (100 MHz, $CDCl_3$): δ 56.19 (CH_3), 56.32 (CH_3), 61.09 (CH_3), 84.28 (C), 86.13 (C), 90.87 (C), 95.85 (C), 108.98 (CH), 109.26 (CH), 109.78 (C), 116.67 (C), 116.89 (C), 116.99 (C), 126.71 (CH), 153.26 (C). Anal. Calcd for $C_{30}H_{23}F_5O_6$: C, 62.72; H, 4.04. Found: C, 62.84; H, 4.30%. HRMS ($M^+ + 1$). Calcd for $C_{30}H_{24}F_5O_6$: 575.149305. Found: 575.149500.

β,β-Bis(4-butyl-2,3,5,6-tetrafluorophenylethynyl)-3,4,5-trimethoxystyrene [9]. The title compound was synthesized using the same procedure as was **8**; however β,β-dibromo-3,4,5-trimethoxystyrene **5** and 1-ethynyl-4-butyltetrafluorobenzene **3**, were used as starting materials. The title compound (green solid) was isolated in 31%: mp 137–138 °C. ^{1}H NMR (400 MHz, $CDCl_3$): δ 0.93–0.97 (t, 6H), 1.34–1.43 (sextet, 4H), 1.56–1.63 (pentet, 4H), 2.73–2.77 (t, 4H), 3.88 (s, 6H), 3.91(s, 3H), 7.207 (br s, 2H), 7.213 (br s, 1H). ^{13}C NMR (50 MHz, $CDCl_3$): δ 13.66 (CH_3), 22.30 (CH_2), 22.86 (CH_2), 32.29 (CH_2), 56.11(CH_3), 61.02 (CH_3), 96.84 (C), 99.55 (C), 100.04 (C), 106.83 (CH), 114.05 (C), 130.15 (C), 140.18 (C), 145.95 (CH), 153.1 (C), 156.76 (C) and a series of broad peaks in the aromatic region (Ar C–F). ^{19}F NMR (376 MHz, $CDCl_3$): δ −154.40 (sm, 2F), −144.84 (sm, 2F), (−138.32)–(−138.24) (t, 2F), −137.80 (sm, 2F). Anal. Calcd for $C_{35}H_{30}F_8O_3$: C, 64.61; H, 4.65. Found: C, 64.80; H, 4.71%.

Fluorescence decay time measurements

All fluorescence decay times were measured by Time Correlated Single Photon Counting (TCSPC). A mode locked Ti:sapphire laser (model 3955, Spectra-Physics) was pumped with a frequency doubled Nd:YAG laser (Millenia Vs, Spectra-Physics) to produce the tunable fundamental beam (wavelength range from 710–980 nm) with a pulse width of about 80–100 fs and a repetition frequency of 80.2 MHz. The fundamental beam was directed into a pulse selector (APE, Berlin) to reduce the repetition frequency to 1 MHz. The fundamental beam output of the pulse selector was directed into the Flexible Harmonic Generator (FHG, Spectra-Physics) resulting in a spectral output for the SHG at 400 nm. A part of the fundamental beam triggered the TCSPC spectrometer FLS 920 from Edinburgh

Table 1 Crystal data and structure refinement for **7**

Empirical formula	$C_{24}H_{11}F_5$
Formula weight	394.33
Temperature	150(2) K
Wavelength	0.56086 A
Crystal system, space group	Monoclinic, $P2_1$
Unit cell dimensions	a = 7.6530(4) Å α = 90 deg.
	b = 13.4288(8) Å β = 94.340(2) deg.
	c = 8.9323(2) Å γ = 90 deg.
Volume	915.35(8) Å^3
Z, Calculated density	2, 1.431 Mg m^3
Absorption coefficient	0.071 mm^{-1}
F(000)	400
Crystal size	0.3 × 0.2 × 0.25 mm
Theta range for data collection	1.80 to 20.00 deg.
Limiting indices	$-9 \le h \le 9$, $-16 \le k \le 15$,
	$-10 \le l \le 9$
Reflections collected/unique	5804/3144 [R(int) = 0.0374]
Completeness to θ = 20.00	99.9%
Refinement method	Full-matrix least-squares on F^2
Data/restraints/parameters	3144/1/302
Goodness-of-fit on F^2	1.099
Final R indices [$I > 2\sigma(I)$]	$R1$ = 0.0545, $wR2$ = 0.1480
R indices (all data)	$R1$ = 0.0674, $wR2$ = 0.1714
Absolute structure parameter	0.2(17)
Largest diff. peak and hole	0.590 and −0.200 e Å^{-3}

Instruments (equipped with single-beam monochromator) using a trigger diode (OCF 400, Becker & Hickel). The FLS 920 is equipped with a TCC 900 card, which incorporates all of the timing electronics for TCSPC. A disk-anode MCP-PMT (ELDY, Europhoton) was used as detector. All fluorescence decay curves were measured in L-geometry. With the setup described, the instrumental response was 100 ps. The fluorescence decay times were calculated by iterative convolution. The software was provided from Edinburgh Instruments as part of the FLS 920. All low temperature measurements were performed using an Oxford Cryostat.

X-Ray crystallography

Preliminary examination and data collection were carried out with Ag-Kα using a Bruker AXS SMART platform diffractometer. Intensity data were collected using three different φ settings and 0.3° increment ω scans, $2\theta < 40°$, which corresponds to more than a hemisphere of data. Data integration was carried out with SAINT,[18] and corrections for absorption and decay were applied using SADABS.[19] Solution was by direct methods and refinement by full matrix least squares[20] on F^2 using all 3144 unique data. The final refinement included anisotropic thermal parameters for non-hydrogen atoms and all hydrogen atoms with isotropic thermal parameters. The refinement converged to $wR_2 = 0.1480$ (for F^2, all data) and $R_1 = 0.0545$ (F, 3144 reflections with $I > 2\sigma(I)$). The crystal data and structure refinement of **7** is presented in Table 1. The bond lengths and angles are shown in Table 2.

Results and discussion

The nature and type of substitution are key factors in determining the emission characteristics of Y-enynes. Therefore, Y-enynes **7**–**9** were prepared from pentafluorobenzaldehyde and 3,4,5-trimethoxybenzaldehyde (Scheme 1). Pentafluorobenzaldehyde **1** and 3,4,5-trimethoxybenzaldehyde **4** were converted to β,β-dibromopentafluorostyrene **2** and β,β-dibromo-3,4,5-trimethoxystyrene **5**, respectively, *via* the Corey–Fuchs reaction.[21] Reaction of **2** and **5** with n-BuLi lead to 1-ethynyl-4-butyltetrafluorobenzene **3** and 1-ethynyl-3,4,5-trimethoxybenzene **6**, respectively.[16] Sonogashira[22] couplings of **2** and phenylacetylene, **2** and **6**, **5** and **3** resulted in β,β-bis(phenylethynyl)pentafluorostyrene **7**, β,β-bis(3,4,5-trimethoxyphenylethynyl)pentafluorostyrene **8** and β,β-bis(4-butyl-2,3,5,6-tetrafluorophenylethynyl)-3,4,5-trimethoxystyrene **9**, respectively.

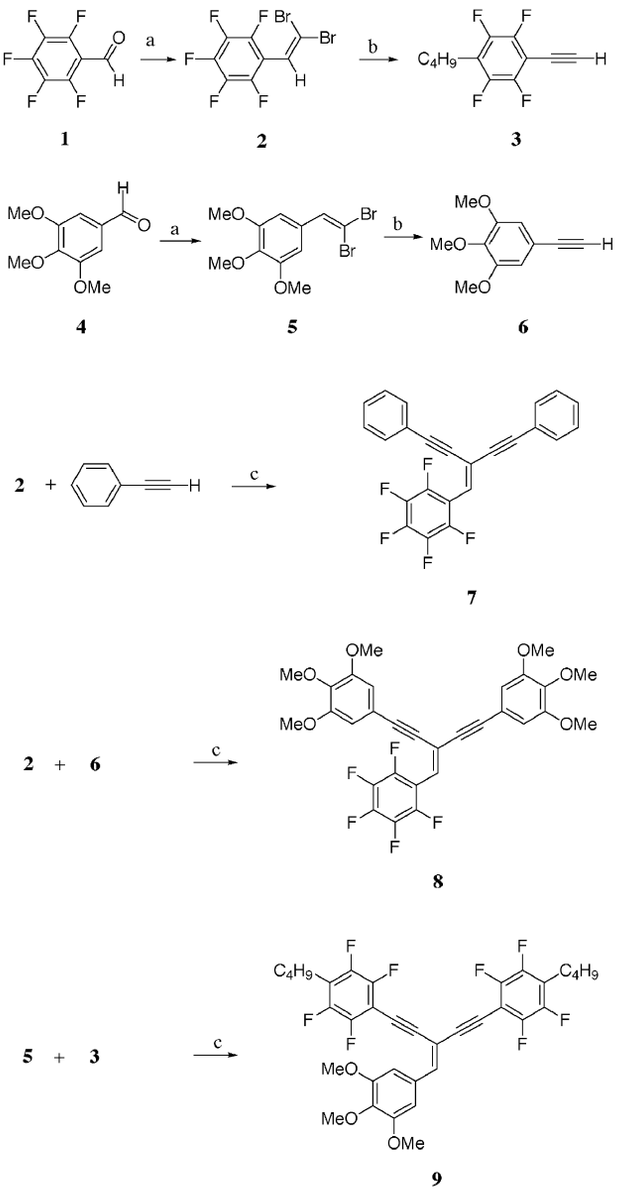

Scheme 1 Synthesis of Y-enynes **7**, **8** and **9**. (a) CBr_4, PPh_3, CH_2Cl_2, 0 °C, argon, 5 h; (b) n-BuLi, THF, −78 °C, argon, 5 h; (c) $Pd(PPh_3)_2Cl_2$, CuI, THF, NEt_3, 70 °C, argon, 24 h.

In Y-enyne **7**, the pentafluorophenyl substituent functions as an electron withdrawing moiety not mesomerically incorporated into the conjugated system. Y-enynes **8** and **9** bearing additional methoxy groups as electron donating substituents were constructed in which the substitution pattern is approximately mirrored allowing comparison in the function of the substituted Y-enyne moiety regarding formation of an intramolecular charge transfer state (**ICT**). Multiple fluorine substitution is important for **ICT**-formation particularly if the compounds are to be used as fluorescent probes.[9]

X-Ray investigations of **7** showed it is not planar.[8a,23] The X-ray crystal structure of **7** (Fig. 1) confirms its chemical structure. This structure shows that the pentafluorophenyl ring is almost parallel to one of the two remaining phenyl rings (dihedral angle of the mean plane of the pentafluorophenyl ring and that having C_{19} is 1.3°) and almost perpendicular to the third phenyl ring (dihedral angle of the mean plane of the pentafluorophenyl ring and that having C_{11} is 94.1°).

Coates *et al.*[24] have reported that phenyl-perfluorophenyl stacking interactions can be used to align molecules in crystals for the topochemical [2 + 2] photodimerization and

Table 2 Bond lengths [Å] and angles [°] for **7**

F(1)–C(2)	1.336(4)	F(2)–C(3)	1.342(5)	F(3)–C(4)	1.341(4)
F(4)–C(5)	1.328(5)	F(5)–C(6)	1.339(4)	C(1)–C(2)	1.389(6)
C(1)–C(6)	1.395(6)	C(1)–C(7)	1.472(4)	C(2)–C(3)	1.384(5)
C(3)–C(4)	1.382(6)	C(4)–C(5)	1.359(6)	C(5)–C(6)	1.384(5)
C(7)–C(8)	1.330(5)	C(8)–C(9)	1.435(5)	C(8)–C(17)	1.445(4)
C(9)–C(10)	1.216(5)	C(10)–C(11)	1.404(6)	C(11)–C(12)	1.405(6)
C(11)–C(16)	1.409(6)	C(12)–C(13)	1.356(7)	C(13)–C(14)	1.387(8)
C(14)–C(15)	1.396(8)	C(15)–C(16)	1.352(7)	C(17)–C(18)	1.196(4)
C(18)–C(19)	1.442(4)	C(19)–C(24)	1.383(6)	C(19)–C(20)	1.391(6)
C(20)–C(21)	1.408(6)	C(21)–C(22)	1.373(8)	C(22)–C(23)	1.365(8)
C(23)–C(24)	1.392(6)				
C(2)–C(1)–C(6)	116.2(3)	C(2)–C(1)–C(7)	119.0(4)		
C(6)–C(1)–C(7)	124.7(4)	F(1)–C(2)–C(3)	117.9(3)		
F(1)–C(2)–C(1)	119.9(3)	C(3)–C(2)–C(1)	122.2(3)		
F(2)–C(3)–C(4)	119.8(3)	F(2)–C(3)–C(2)	120.8(4)		
C(4)–C(3)–C(2)	119.4(4)	F(3)–C(4)–C(5)	119.9(4)		
F(3)–C(4)–C(3)	119.8(4)	C(5)–C(4)–C(3)	120.3(3)		
F(4)–C(5)–C(4)	120.6(3)	F(4)–C(5)–C(6)	119.6(4)		
C(4)–C(5)–C(6)	119.8(4)	F(5)–C(6)–C(5)	118.3(3)		
F(5)–C(6)–C(1)	119.5(3)	C(5)–C(6)–C(1)	122.1(3)		
C(8)–C(7)–C(1)	125.6(4)	C(7)–C(8)–C(9)	121.9(3)		
C(7)–C(8)–C(17)	121.5(3)	C(9)–C(8)–C(17)	116.5(3)		
C(10)–C(9)–C(8)	179.1(4)	C(9)–C(10)–C(11)	175.9(4)		
C(10)–C(11)–C(12)	119.5(4)	C(10)–C(11)–C(16)	122.6(4)		
C(12)–C(11)–C(16)	117.9(4)	C(13)–C(12)–C(11)	120.7(4)		
C(12)–C(13)–C(14)	120.9(5)	C(13)–C(14)–C(15)	119.2(5)		
C(16)–C(15)–C(14)	120.4(5)	C(15)–C(16)–C(11)	121.1(4)		
C(18)–C(17)–C(8)	174.4(4)	C(17)–C(18)–C(19)	177.6(4)		
C(24)–C(19)–C(20)	119.2(3)	C(24)–C(19)–C(18)	119.7(4)		
C(20)–C(19)–C(18)	121.1(4)	C(19)–C(20)–C(21)	119.5(4)		
C(22)–C(21)–C(20)	120.2(4)	C(23)–C(22)–C(21)	120.4(3)		
C(22)–C(23)–C(24)	120.1(5)	C(19)–C(24)–C(23)	120.6(4)		

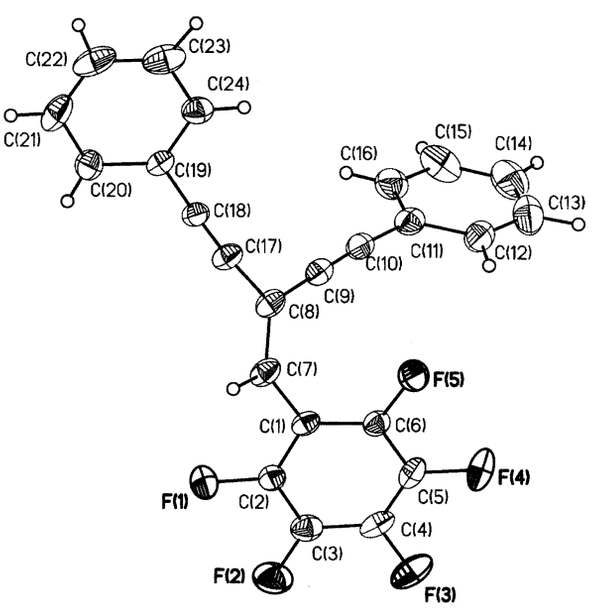

Fig. 1 ORTEP of **7** at 150 K (ellipsoids at 50% probability).

photopolymerization of olefinic compounds, as well as the polymerization of diynes.[25] The X-ray structure of **7** reveals face-to-face stacking interactions between the phenyl and perfluorophenyl groups of different molecules. These interactions result in high order stacking of the molecules in the solid state. The pentafluoro phenyl ring of one molecule stacks above a phenyl ring of another molecule forming a "ladder" (Fig. 2a). The distance between the stacked rings is 3.7 Å. Several "ladders" stack so that a phenyl ring is stacked between two pentafluorophenyl rings while a pentafluorophenyl ring is stacked between two phenyl rings (Fig. 2b). This stacking results in the formation of channels along the aromatic rings, 2.76 Å in diagonal (Fig. 2c).

Moore and co-workers[26] first reported acetylene–arene π–π interactions as a driving force for aggregation of phenylacetylene macrocycles. These authors reported that π–π interactions maximized when the triple bond lies parallel to the aromatic plane (tilt angle, θ, is 90°), and the distance between the aromatic centroid and the center of the carbon–carbon triple bond lies within 10 Å.[26] Solid stacking of Y-enyne **7**, as revealed by the X-ray measurement, predicts such interactions. One of the two acetylene carbon–carbon triple bonds in molecule A has a tilt angle θ_1 = 88.7° with respect to the pentafluorophenyl ring of molecule B[27] (Fig. 3); this triple bond has the same tilt angle with the molecule above it (not shown for simplicity). The other carbon–carbon triple bond in molecule A has a tilt angle θ_2 = 30.2° with the pentafluorophenyl ring of molecule B and tilt angle θ_3 = 31.5° with the phenyl ring of molecule C. Furthermore, we propose attractive interaction between the fluorine atoms (the most electronegative atoms in the periodic table) in molecule B and the p-orbitals (electron rich) of the acetylene in molecule A also contribute to the solid stacking. Therefore, the coulombic interactions and the acetylene–arene π–π interactions, in addition to the fluorine–π interactions, contribute to the high order stacking of **7**.

The X-ray structure confirms that the conjugation of the chromophore of **7** is distorted in the solid state. The hydrogen bonded to C_7 (H_7) is 45° out of the plane (Fig. 2b) of the pentafluoro ring (dihedral angle of ($H_7C_7C_1$) and the mean plane of the pentafluorophenyl ring is 135°). This requires the p-orbital of C_7 to be at 45° with that of C_1 (Fig. 4). Therefore, the pentafluoro ring is in "semi" conjugation with the rest of the chromophore.

The absorption spectra of **7**, **8** and **9** in CH_3CN are plotted in Fig. 5. The shape of the absorption spectra of **7** and **8** appear similar. The additional methoxy substituents of **7** (as in **8**) resulted in a slight bathochromic shift of the absorption maximum indicating stabilization of the excited state. Compound **9**, though the general structure of the absorption is similar to **8** is different in both ε and λ_{max}^{abs}, Table 3. Though **9** has fewer methoxy substituents than **8**, its absorption spectrum exhibits the largest bathochromic shift (45 nm). Presumably, Y-enyne **9** is less sterically hindered than **8** resulting in more stabilization of the π-system of **9**.[28]

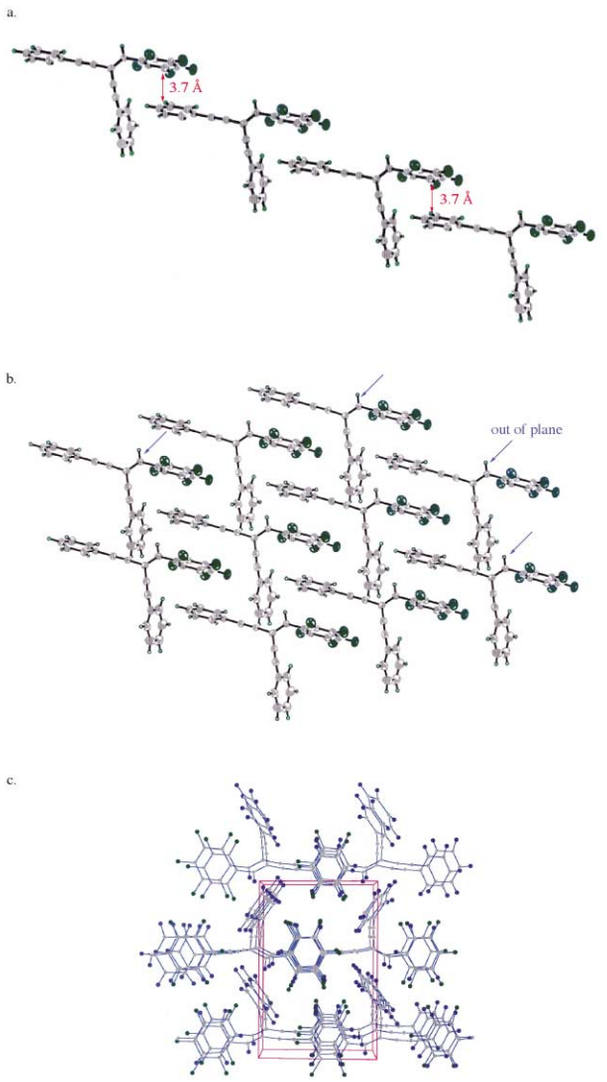

Fig. 2 Stacking of **7**. (a) Line of molecules; (b) a layer of molecules; (c) view of the unit cell along the *a* axis.

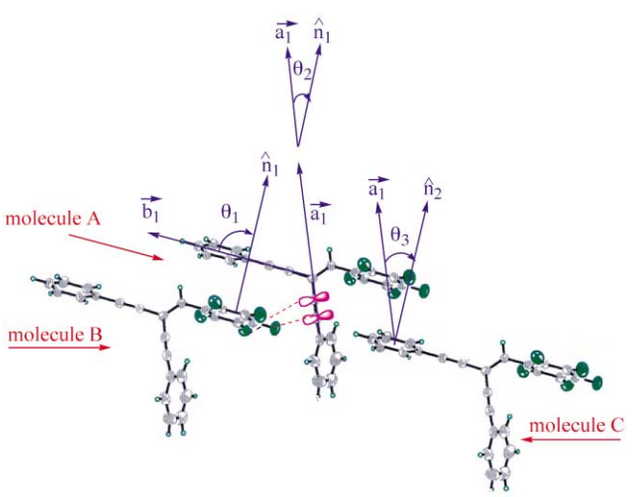

Fig. 3 Acetylene–arene π–π and fluorine–π interactions in **7**; a_1, b_1 and n_1 are the axis and normal of molecule A.

No significant solvatochromic behavior was observed for the absorption spectra when switching from the more polar acetonitrile to the less polar cyclohexane for **7** and **9**; however, a blue shift (hypsochromic shift) of 20 nm was observed for **8** on going from cyclohexane to acetonitrile (Table 3). This is the result of better ground state solvation in nonpolar solvents and

Table 3 Absorption data for **7**, **8**, and **9** in acetonitrile (CH_3CN) and cyclohexane (CH)

Compound	Solvent	λ_{max}^{abs}/nm	ε/M^{-1} cm^{-1}
7	CH_3CN	305	26 600
	CH	309	28 600
8	CH_3CN	323	29 700
	CH	343	27 800
9	CH_3CN	368	32 100
	CH	373	35 800

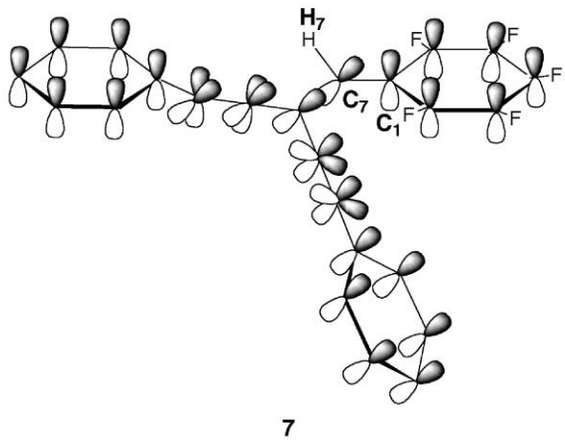

7

Fig. 4 The distorted conjugation of **7**.

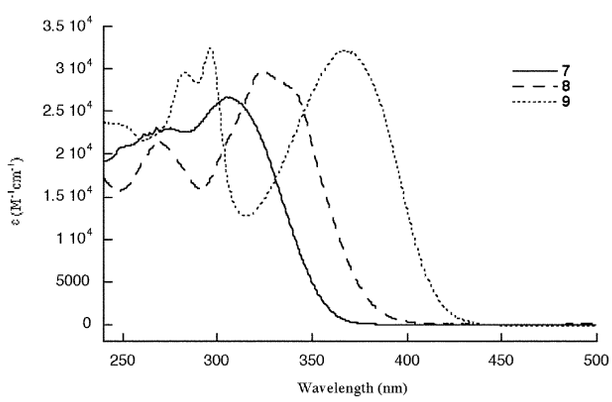

Fig. 5 Absorption of **7**, **8** and **9** in CH_3CN.

solvent induced geometry changes. In other words, the π-system may become more planar by changing the surrounding solvent. Y-enynes **7**–**9** are photostable.

Fluorescence measurements in different solvents showed no solvatochromism for **7** (Fig. 6a) but significant bathochromic shifts for **8** (Fig. 6c) and **9** (Fig. 6b), Table 4. Y-enyne **8**, which bears two electron donating phenyl groups on the acetylene moiety, exhibits the largest bathochromic shift, Fig. 6c and Table 4, indicating both the Y-enyne bridge and the number of electron donating substituents affect the strength of solvatochromism. The distinct substitution pattern in **8** and **9** affects the photophysical behavior because the electron density of the aromatic system differs.

The solvatochromism observed for **8** and **9** supports **ICT**-formation. Dipole moment changes ($\Delta\mu$), evaluated from the slope of the Lippert–Mataga equation, are the largest for **8**, Table 4. Both the solvatochromic slope and $\Delta\mu$ are reasonable when compared with other solvatochromic fluorophores.[11] Our results clearly show that the structural donor–acceptor pattern of **8** is more appropriate in order to get a larger solvatochromic slope as compared to **9**. In other words, fluorescent Y-enynes with solvatochromic properties should bear the electron-donating moiety at the aromatic attached to the acetylene bond

Table 4 Emission data, solvatochromic slope of the Lippert–Mataga equation ($1/hc2\pi\varepsilon_0(\mu_e(\mu_e - \mu_g)/\rho^3)$) and change of dipole moment between S_0 and S_1 ($\Delta\mu$) for **7**, **8**, and **9** in cyclohexane (CH) and acetonitrile (CH_3CN)

Compound	Solvent	φ_f	λ_{max}^{fl} /nm	$1/2hc\pi\varepsilon_0(\mu_e(\mu_e - \mu_g)/\rho^3)$ /cm^{-1}	$\Delta\mu$ (D)
7	CH	0.004	410	0	0
	CH_3CN	0.006	410		
8	CH	0.015	456	−10,800	9.6
	CH_3CN	0.011	550		
9	CH	0.005	439	−6,400	6.9
	CH_3CN	0.006	483		

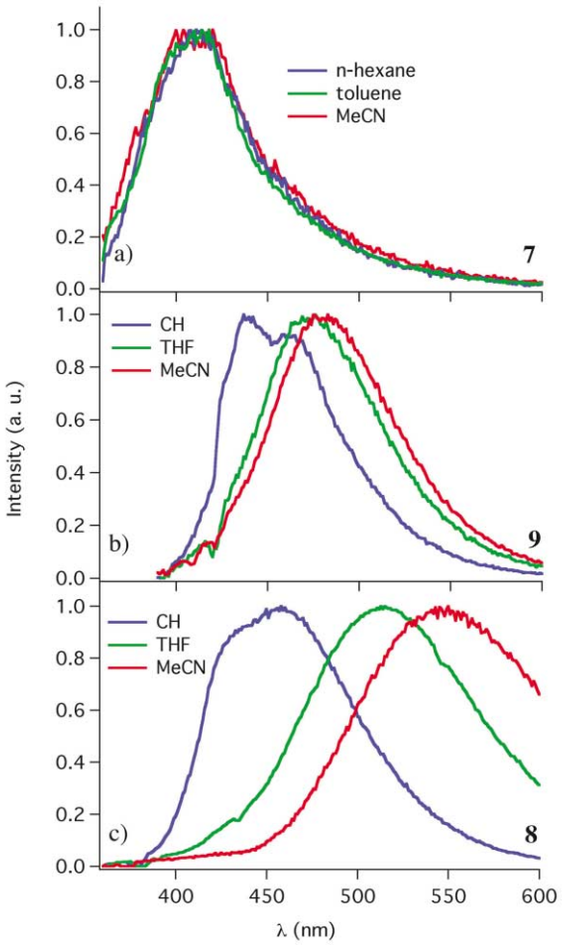

Fig. 6 Normalized emission of **7** (a; top), **9** (b; middle) and **8** (c; bottom) in solvents of different polarity (CH = cyclohexane, THF = tetrahydrofuran, MeCN = acetonitrile). λ_{exc} (**7**) = 320 nm; λ_{exc} (**8**) = 335 nm; λ_{exc} (**9**) = 375 nm.

while the aromatic attached to the double bond should have electron withdrawing groups.

Effective nonradiative deactivation competes either with **ICT**-formation or radiative deactivation of the locally excited state (**LE**). Low fluorescence quantum yields were measured for **7**–**9** in ordinary solvents at room temperature, Table 4. Isomerization of the double bond is the main pathway for nonradiative deactivation. The efficiency of this can be reduced in frozen organic glasses because this process suffers from increasing viscosity and results in an increase of the fluorescence decay time-τ_f, Fig. 7. The fluorescence decay time of **9** decreases in methyltetrahydrofuran (MTHF) from 2.1 ns at 77 K to 0.17 ns at 160 K and finally to 0.11 ns at 200 K. These data clearly show the competition between radiative and nonradiative processes. The higher the temperature of the surrounding solvent, the lower the solvent viscosity and therefore the better the efficiency for nonradiative deactivation. The latter is caused by double bond rotation in the excited state.

Furthermore, temperature dependent ^{1}H-NMR (400 MHz) measurements of **9** in $CDCl_3$ (freezing point = −63.5 °C) indicated efficient single bond rotation. At 25 °C, rapid rotation of the trimethoxyphenyl ring of **9** averages the chemical shifts of the two *meta* OCH_3 groups (3.88 ppm, 6 H) and differentiates them from the *para* OCH_3 (3.91 ppm, 3H). The three MeO groups in **5** collapse into one peak at 3.87 ppm. The MeO groups in **6** coalesce at 3.86 ppm. However, the *para* and *meta* MeO groups in **9** differ due to the extended conjugation with the fluorinated rings. When the temperature is lowered, the rotation around the single bond of the trimethoxyphenyl ring slows moving the OCH_3's closer in chemical shift until, at −50 °C, all OCH_3's have the same chemical shift, 3.93 ppm (Fig. 8). We attribute this to the absence of conjugation due to frozen rotational conformation in which the trimethoxyphenyl ring is perpendicular to the fluorinated rings (Fig. 9). Therefore it is not affected by the fluorinated rings and behaves as it does in starting material **5**.

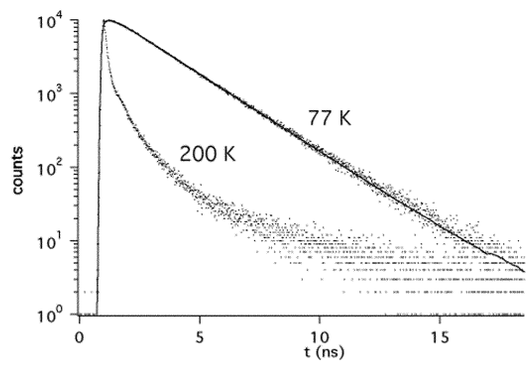

Fig. 7 Fluorescence decay of **9** in methyltetrahydrofuran at 77 K and 200 K.

The general photophysical scheme for the Y-enynes **8** and **9** is depicted in Scheme 2. The **LE** competitively decays either into a radiationless decaying component of biradicaloid nature (formed by double bond rotation) or a species exhibiting **ICT**-properties. These compounds are therefore viscosity (sensitive response upon change of viscosity) and polarity (sensitive response upon change of polarity) dependent fluorescent probes.

The dipole moments of the excited states were determined using the Lippert–Mataga treatment, eqn. (1).[29] Ground state dipole moments were used as obtained from quantum chemical calculations by using the AM1 Hamiltonian. Most of the solvents, with the exception of toluene, resulted in a reasonable correlation between the emission energy and the solvent polarity function Δf, Fig. 10. Toluene can π-stack with the fluorinated moiety of the fluorophore and may result in an additional energetic stabilization that is not included in the Lippert–Mataga theory.

$$\nu_{CT} = const. - \frac{1}{4\pi hc\varepsilon_0}.\frac{2}{\rho^3}.\mu_{CT}^{exc}(\mu_{CT}^{exc} - \mu_{CT}^{GS(FC)}) \times \Delta f \qquad (1)$$
$$\nu_{CT} = const. - m \times \Delta f$$

Equation (1) states that the emission wavenumber ν_{CT} in a specific solvent is proportional to the solvent polarity

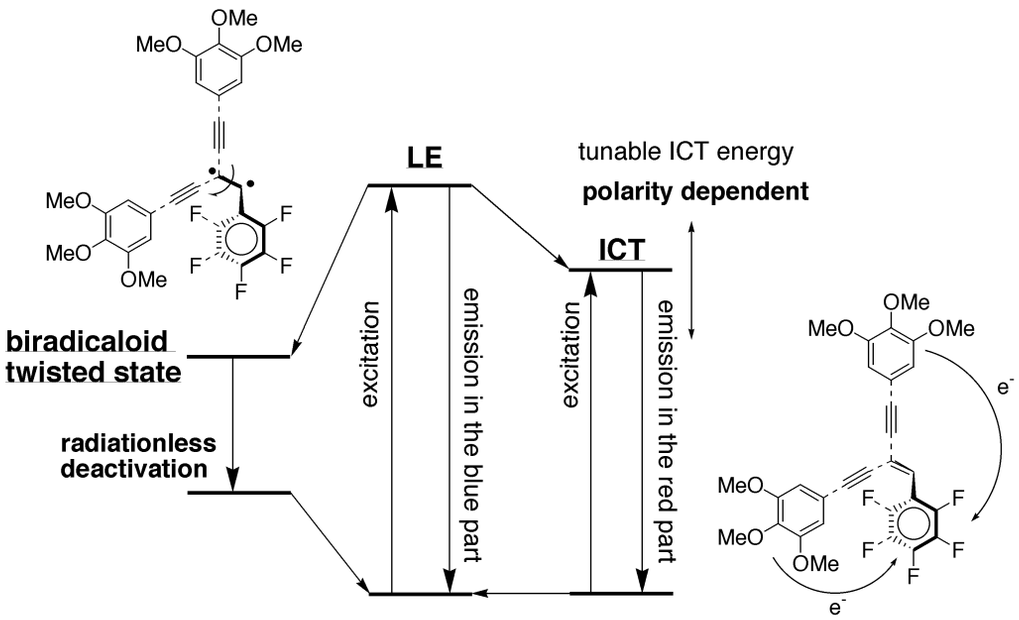

Scheme 2 Possible reaction pathways in the excited state of donor–acceptor substituted Y-enynes **8** and **9**.

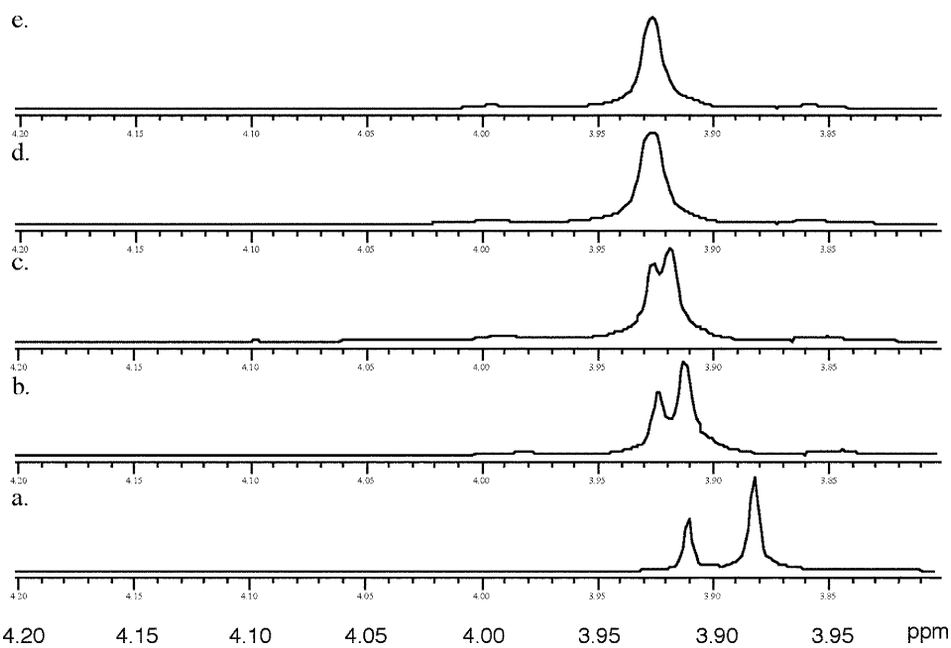

Fig. 8 ^{1}H-NMR of **9** in $CDCl_3$ at different temperatures: (a) 25 °C; (b) −35 °C; (c) −45 °C; (d) −50 °C; (e) −55°C.

parameter Δf, which is defined by Eqn. (2), in which ε is the relative permitivitty and n is the optical refractive index of the solvent. In equation (1), ε_0 is the permittivity in vacuum, ρ is the Onsager radius,[30] h is the Planck's constant, μ_{CT}^{exc} is the dipole moment of the CT in the excited state, and $\mu_{CT}^{GS(FC)}$ is the dipole moment of the ICT in the ground state with Franck Condon geometry.

$$\Delta f = \frac{\varepsilon - 1}{2\varepsilon + 1} - \frac{1}{2}.\frac{n^2 - 1}{2n^2 + 1} \qquad (2)$$

Conclusions

An approach to the development of fluorescent probes from fluorinated Y-enynes is reported. Different substitution patterns in the Y-enynes result in distinct solvatochromic behavior. Donor substituted Y-enynes **8** and **9** exhibit solvatochromism upon change of solvent polarity. Y-enyne **8** showed the largest solvatochromic shift (94 nm bathochromic shift) upon changing solvent from cyclohexane to acetonitrile. A smaller solvatochromic response (44 nm bathochromic shift) was observed for **9**. The solvatochromic behavior in **8** and **9** supports the formation of an intramolecular charge transfer (ICT) state. Compounds **8** and **9** are viscosity and polarity dependent fluorophores. Y-enyne **7** stacks in the solid state due to coulombic, actetylene–arene, and fluorine–π interactions. The conjugation of **7** is distorted.

Acknowledgements

The authors are grateful to Professor G. S. Hammond, Professor T. H. Kinstle, and Professor A. A. Pinkerton for insightful discussions. B. R. K. thanks the McMaster Endowment for a research fellowship. This work was supported by NSF (Grant # DMR-0091689).

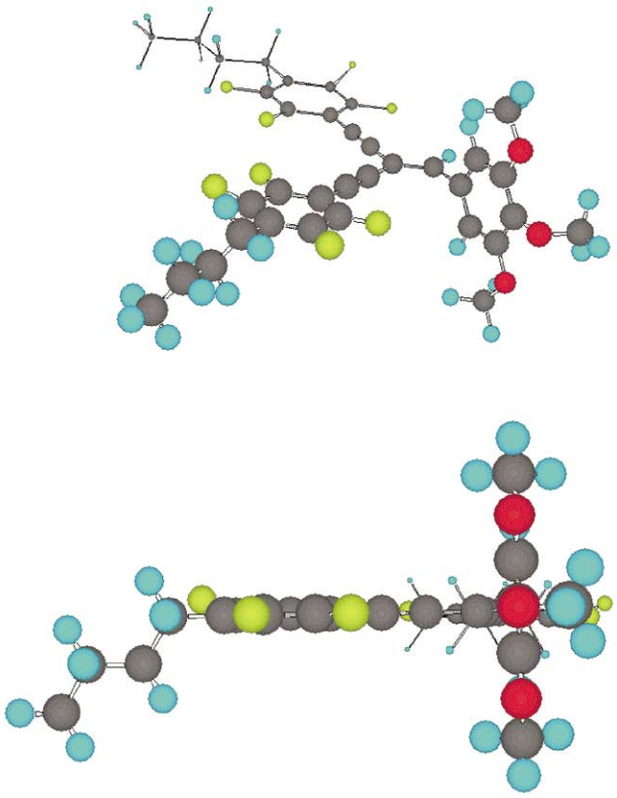

Fig. 9 The proposed configuration of **9** at −50 °C.

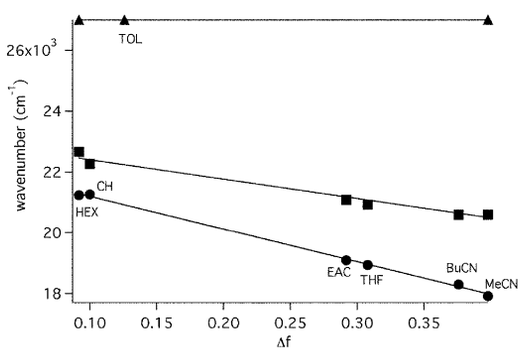

Fig. 10 Lippert-Mataga plot according to eq. 1 for compounds **7**, **8** and **9** in solvents of different polarity (CH = cyclohexane, HEX = *n*-hexane, TOL = toluene, EAC = ethyl acetate, THF = tetrahydrofuran, BuCN = butyronitrile, MeCN = acetonitrile); · for **7**, ● for **8**, and ■ for **9**.

References

1 Contribution # 470 from the Center for Photochemical Sciences.

2 For reviews, see: (*a*) P. Suppan, Invited review. Solvatochromic shifts. The influence of the medium on the energy of electronic states, *J. Photochem. Photobiol., A*, 1990, **50**, 293–330; (*b*) C. Reichardt, Solvatochromic Dyes as Solvent Polarity Indicators, *Chem. Rev.*, 1994, **94**, 2319–2358.

3 W. F. Jager, A. A. Volkers and D. C. Neckers, Solvatochromic Fluorescent Probes for Monitoring the Photopolymerization of Dimethacrylates, *Macromolecules*, 1995, **28**, 8153–8158.

4 B. Strehmel, J. H. Malpert, A. M. Sarker and D. C. Neckers, New Intramolecular Fluorescence Probes That Monitor Photoinduced Radical and Cationic Cross-Linking, *Macromolecules*, 1999, **32**, 7476–7482.

5 (*a*) Z. J. Wang, J. C. Song, R. Bao and D. C. Neckers, Fluorescence probes for monitoring polymerization processes, *J. Polym. Sci. Part B: Polym. Phys.*, 1996, **334**, 325–333; (*b*) J. C. Song and D. C. Neckers, Characterization of photocurable coatings using fluorescence probes, *Polym. Eng. Sci.*, 1996, **36**, 394–402; (*c*) S. Hu, R. Popielarz and D. C. Neckers, Fluorescence Probe Techniques (FPT) for Measuring the Relative Efficiencies of Free-Radical Photoinitiators, *Macromolecules*, 1998, **31**, 4107–4113.

6 J.-P. Fouassier, in *Photoinitiation, Photopolymerization, and Photocuring: Fundamentals and Applications*, Hanser Publications, CincinnatiOH, 1995.

7 (*a*) Y. Zhao, R. McDonald and R. R. Tykwinski, Study of cross-conjugated *iso*-polytriacetylenes and related oligoenynes, *J. Org. Chem.*, 2002, **67**, 2805–2812 and references therein; (*b*) G. T. Hwang, H. S. Son, J. K. Ku and B. H. Kim, Novel fluorophores: efficient synthesis and photophysical study, *Org. Lett.*, 2001, **3**, 2469–2471; (*c*) L. Fomina and R. Salcedo, Synthesis and polymerization of β,β-dibromo-4-ethynylstyrene; preparation of a new polyconjugated, hyperbranched polymer, *Polymer*, 1996, **37**, 1723–1728; (*d*) L. Fomina, P. Guadarrama, S. Fomine, R. Salcedo and T. Ogawa, Synthesis and characterization of well-defined fully conjugated hyperbranched oligomers of β,β-dibromo-4-ethynylstyrene, *Polymer*, 1998, **39**, 2629–2635; (*e*) L. Fomina, H. Allier, S. Fomine, R. Salcedo and T. Ogawa, Synthesis and molten-state polymerization of some novel conjugated diacetylenes, *Polym. J. (Tokyo)*, 1995, **27**, 591–600; (*f*) S. Fomine, L. Fomina, H. Q. Florentino, J. M. Mendez and T. Ogawa, Novel polymers containing discrete conjugated units, produced by the Heck reaction, *Polym. J. (Tokyo)*, 1995, **27**, 1085–1093; (*g*) L. Eshdat, H. Berger, H. Hopf and M. Rabinovitz, Anionic Cyclization of a Cross-Conjugated Enediyne, *J. Am. Chem. Soc.*, 2002, **124**, 3822–3823.

8 (*a*) B. R. Kaafarani, A. A. Pinkerton and D. C. Neckers, High order stacking of a perfluoro 'Y-enyne', *Tetrahedron Lett.*, 2001, **42**, 8137–8139; (*b*) B. R. Kaafarani and D. C. Neckers, Photocyclization of a conjugated triaryl 'Y-enyne', *Tetrahedron Lett.*, 2001, **42**, 4099–4102; (*c*) B. R. Kaafarani, B. Wex, J. A. K. Bauer and D. C. Neckers, Photocyclization of a naphthyl substituted Y-enyne, *Tetrahedron Lett.*, 2002, 8227–8230.

9 B. Strehmel, A. M. Sarker, J. H. Malpert, V. Strehmel, H. Seifert and D. C. Neckers, Effect of aromatic ring substitution on the optical properties, emission dynamics, and solid state behaviour of fluorinated oligophenylenevinylenes, *J. Am. Chem. Soc.*, 1999, **121**, 1226–1236.

10 B. Strehmel, K. B. Henbest, A. M. Sarker, J. H. Malpert, D. Y. Chen, M. A. J. Rodgers and D. C. Neckers, Ion-induced manipulation of photochemical pathways in crown ether compounds based on fluorinated oligophenylenevinylenes: the border between ultrafast photoswitches and photoproduced nanomaterials, *J. Nanosci. Nanotechnol.*, 2001, **1**, 107–124.

11 B. Strehmel, Fluorescence Probes for Material Science, in *Advanced Functional Molecules and Polymers*, ed. H. S. Nalwa, Gordon and Breach Publishing Group, Amsterdam, 2001, Vol. 3, pp. 299–384.

12 L. Gobbi, N. Elmaci, H. P. Lüthi and F. Diederich, N,N-Dialkylaniline-substituted tetraethynyl-ethenes: a new class of chromophores possessing an emitting charge-transfer state. Experimental and computational studies, *ChemPhysChem*, 2001, **2**, 423–433 and references therein.

13 W. R. Dawson and M. W. Windsor, Fluorescence yields of aromatic compounds, *J. Phys. Chem.*, 1968, **72**, 3251–3260.

14 H. Sanyo and F. J. Hirayama, Actinometric determination of absolute fluorescence quantum yields, *Phys. Chem.*, 1983, **87**, 83–89.

15 D. Venkatesan, M. Yoneda and M. Ueda, Conjugated polymers for nonlinear optics. 1. Synthesis and properties of poly(arylene-ethynylenevinylene)s, *React. Funct. Polym.*, 1996, **30**, 341–352.

16 N. J. Lawrence, A. F. Ghani, L. A. Hepworth, J. A. Hadfield, A. T. McGown and R. G. Pritchard, The synthesis of (E)- and (Z)-combretastatins A-4 and a phenanthrene from Combretum caffrum, *Synthesis*, 1999, 1656–1660.

17 S. Huang and J. M. Tour, Rapid bi-directional synthesis of oligo-(1,4-phenylene ethynylene)s, *Tetrahedron Lett.*, 1999, **40**, 3347–3350.

18 Bruker (1999). SMART (Ver. 5.05) and SAINT-Plus (Ver. 7.08). Bruker AXS Inc, Madison, Wisconsin, USA.

19 G. M. Sheldrick, 1996 . SADABS. *Program for the empirical Absorption correction of Area detector data*, University of Göttingen, Germany.

20 G. M. Sheldrick, 1996 . SADABS. *Program for the empirical Absorption correction of Area detector data*, University of Göttingen, Germany.

21 E. J. Corey and P. L. Fuchs, Synthetic method for conversion of formyl groups into ethynyl groups (RCHO .far. RC .idn. CH or RC .idn. CR1), *Tetrahedron Lett.*, 1972, 3769–3772.

22 K. Sonogashira, Y. Tohda and N. Hagihara, Convenient synthesis of acetylenes. Catalytic substitutions of acetylenic hydrogen with bromo alkenes, iodo arenes, and bromopyridines, *Tetrahedron Lett.*, 1975, 4467–4470.

23 The crystallographic data is deposited at the Cambridge Crystallographic Data Center (CCDC # 174497).

24 G. W. Coates, A. R. Dunn, L. M. Henling, J. W. Ziller, E. B. Lobkovsky and R. H. Grubbs, Phenyl-perfluorophenyl stacking interactions: topochemical [2+2] photodimerization and photopolymerization of olefinic compounds, *J. Am. Chem. Soc.*, 1998, **120**, 3641–3649.
25 G. W. Coates, A. R. Dunn, L. M. Henling, D. A. Dougherty and R. H. Grubbs, Phenyl-perfluorophenyl stacking interactions: a new strategy for supermolecule construction, *Angew. Chem., Int. Ed.*, 1997, **36**, 248–251.
26 A. S. Shetty, J. Zhang and J. S. Moore, Aromatic π-Stacking in Solution as Revealed through the Aggregation of Phenylacetylene Macrocycles, *J. Am. Chem. Soc.*, 1996, **118**, 1019–1027.
27 The distance between the aromatic centroid of the pentafluorophenyl ring in molecule A and the center of the carbon-carbon triple bond in molecule B is 4.097Å.
28 X-ray structure analysis of **8** and **9** is in progress.
29 (*a*) E. Lippert and W. Z. Lüder, Spectroscopic investigations and dipole measurements on the electron structure of cis- and trans-p-dimethylamino cinnamic acid nitrile and related nitriles, *Z. Physik. Chem. (Frankfurt)*, 1962, **33**, 60–81; (*b*) E. Lippert, Spectroscopic determination of the dipole moment of aromatic compounds in the first excited singlet state, *Z. Elektrochem.*, 1957, **61**, 962–975; (*c*) N. Mataga, Y. Kaifu and M. Koizumi, The solvent effect on fluorescence spectrum. Change of solute-solvent interaction during the lifetime of excited solute molecule, *Bull. Chem. Soc. Jpn.*, 1955, **28**, 690–691; (*d*) N. Mataga, Y. Kaifu and M. Koizumi, Solvent effects upon fluorescence spectra and the developments of excited molecules, *Bull. Chem. Soc. Jpn.*, 1956, **29**, 465–470.
30 L. Onsager, Electric moments of molecules in liquids, *J. Am. Chem. Soc.*, 1936, **58**, 1486–1493.